

**Seagrass Mapping and Human Impact Evaluation
Using Remote Sensing Imagery at Core Banks, North Carolina**

by

Shuyue Li

Dr. Jennifer Swenson, Adviser

April 27, 2018

Master's project submitted in partial fulfillment of the
requirements for the Master of Environmental Management degree in
the Nicholas School of the Environment of
Duke University

Executive Summary

Seagrass Mapping and Human Impact Evaluation Using Remote Sensing Imagery at Core Banks, North Carolina

by

Shuyue Li

4/27/2018

Seagrass, generally referred to as submerged marine plants growing in shallow benthic beds, can provide key ecological services to neighboring habitats in tropical and temperate regions. While seagrasses have been recognized as a priority for conservation efforts worldwide, evidence shows that they are experiencing significant widespread decline. Multiple reasons can cause noticeable seagrass decline, but coastal human population pressures play a most important role, including fishing, aquaculture, introduced exotic species, boating, habitat alteration, etc. This study focused on the damage of boating, which usually occurs when a boat propeller touches either the submerged vegetation or the bay bottom. Propeller scars may lead to direct loss of seagrass and increased susceptibility of seagrass beds to damage from hurricanes.

The goal of this study is to explore the methods for seagrass mapping based on remote sensing imagery, and to evaluate the impact of human activities on seagrass beds. A transect at Core Banks in Beaufort, NC was selected as the study area, which contains seagrass beds consisting of multiple species. A major data source for this study was the imagery surveyed by unoccupied aircraft system (UAS), a technique being increasingly used in environmental studies in recent decades with an advantage of ultrahigh resolution. Four UAS georeferenced color mosaics (2.5- to 3-cm pixel size) collected in June, July, September and October were used for seagrass mapping, analysis of the effect of propeller scars and the recovery of those scars. Another data source was high resolution multispectral satellite imagery (RapidEye, 5-m pixel resolution), which was used for exploring large-area automated seagrass mapping.

The first part of this study was to identify seagrass areas in the UAS images. The classification method applied was Object-Based Image Analysis. Based on the classification results, which were binary images of seagrass versus non-seagrass areas, I manually identified propeller scars and extracted bare patches where the aggregations of non-seagrass pixels were larger than a selected threshold. Object-based classification was performed using Rule-based Feature Extraction in ENVI software. Validated using ~150 random scattered points, the error matrices indicated this classification method had fairly good results. Classified binary images also showed increased seagrass coverage from June to July, followed by a continuous decline in seagrass from September to October.

The second part of this study was edge-effect analysis. A 3-m buffer zone was delineated based on the proximity of extracted scar areas. The percentage coverage of seagrass in scar-affected/non-affected regions over four months was calculated in ArcMap. Over the 113,620 m² study area, the scar-affected zone covered about 60%, while the remainder was not affected. By calculating the percentage coverage of seagrass in the scar-affected/non-affected regions over four months, I found that the seagrass in scar-affected regions had a greater rate of both growth and decline.

The third part was the factors influence propeller scars recovery. A total of 28 scars were selected and categorized into three levels according to their recovery conditions relative to October of last year:

completely recovered, partially recovered and not recovered. During this process, the Visible Atmospheric Resistant Index (VARI) was chosen as the proxy of leaf area index in the visible spectrum, and a relative normalization method was adopted as the alternative solution for radiometric correction. The area-normalized VARI of completely recovered areas was higher than partially or not recovered areas, while the partially or not recovered areas didn't show a significant difference in terms of their recovery speed and timing. Completely recovered areas also had an earlier peak growth season than partially or not recovered areas. The difference in initial conditions before scarring and the discrepancy of species composition can possibly explain this finding, but on-the-ground data is needed for further confirmation.

The fourth part was large area seagrass mapping based on high-resolution multispectral satellite imagery. This study used RapidEye imagery, and a newly developed index, ReGNDVI (replacing the near-infrared band with red-edge band and replacing red band with green band of the NDVI), for a single-thresholding classification. Seagrass beds were found the most distinct spectral signature using the double ReGNDVI transform; this method had 74% total accuracy.

Based on the analysis above, this study makes several key points and recommendations:

- It provides a successful application of Object-Based Classification in classifying coastal submerged areas in UAS images, showing that UAS techniques have potential in monitoring submerged areas as well as conservation of coastal habitats. However, the performance of UASs is dependent on a series of related techniques, especially radiometric correction and spectral resolution. These issues should be addressed in planning stage of similar research or conservation work.
- Through the analysis on propeller scar impact on seagrass, human activities have been proven to have lasting effects on seagrass habitat, since seagrass in scar-affected regions has a greater rate of both growth and decline. The scars in areas with higher density of seagrass are more likely to recover, although this conclusion needs further confirmation with on-the-ground species composition data. This finding does support the management recommendation that human activities should be restricted in vulnerable seagrass habitats, and necessary boating or fishing pathways should only be allowed in areas with a high-density of seagrass, since these areas are less susceptible to propeller scars.
- In addition, this study also shows that automated seagrass mapping is feasible using high-resolution satellite imagery (e.g. RapidEye) and a newly developed index, ReGNDVI (Red Edge-Green NDVI). It has potential for large-area seagrass mapping, and might be useful for conservation of coastal areas.

Contents

Executive Summary	1
1. Introduction	5
1.1 Human Impact on Seagrass.....	5
1.2 Application of Remote Sensing Approach on Seagrass Mapping	6
1.3 Edge Effect of Habitat Fragmentation	7
1.4 Project Objectives	8
2. Methods	8
2.1 Study Site	8
2.2 Data Description	9
2.2.1 Drone-Surveyed RGB Mosaics.....	9
2.2.2 High Resolution RapidEye Satellite Imagery	10
2.3 Analyses.....	11
2.3.1 Object-Based Image Classification	12
2.3.2. Edge-Effect Analysis	12
2.3.3. Recovery Conditions Exploration.....	13
2.3.4 Large Area Seagrass Identification	15
3. Results	16
3.1 Ultrahigh-Resolution Seagrass Mapping	16
3.2 Edge Effect Analysis.....	17
3.3 Recovery Conditions.....	19
3.4 Seagrass Mapping based on New Index	20
4. Discussions	23
4.1 Issues on Analyses Techniques.....	23
4.2 Discussion on Seagrass Recovery	24
5. Conclusions	25
Acknowledgement	26
References	27
Supplementary Materials	28

Figures

Figure 1. Map of study area.	9
Figure 2. Observed water level at Beaufort station during 2017/09/13.	11
Figure 3. Comparison of categorized propeller scars.....	14
Figure 4. Classified binary seagrass images for four months	16
Figure 5. Changes of seagrass coverage within 113620-m ² study area over time in 2017	17
Figure 6. Scar-affected areas versus non-affected areas	18
Figure 7. Changes of seagrass coverage in scar-affected/non-affected areas over time	19
Figure 8. Visible Atmospheric Resistant Index (VARI) of three recovery-level areas in four months	20
Figure 9. Seagrass mapping using RapidEye imagery.....	21
Figure 10. Spectral signature of four classes through four transforms	22

Tables

Table 1. Accuracy assessment matrix of classified images in four months	17
---	----

1. Introduction

1.1 Human Impact on Seagrass

Seagrass, generally referred to submerged marine plants growing in shallow benthic beds, provides key ecological services to neighboring habitats in tropical and temperate regions, including carbon production and export, nutrient transfer and cycling, sediment stabilization, and enhancing biodiversity (Orth, R. J. et al, 2006). While seagrasses have been recognized as a priority for conservation efforts worldwide, evidence shows that they are experiencing significant widespread decline. Multiple reasons can cause noticeable seagrass decline, but coastal human population pressures play a most important role.

Common human activities that impact seagrasses directly include fishing and aquaculture, introduced exotic species, boating and anchoring, and habitat alteration (Duarte, C. M. et al, 2004). This study will focus on the influence of power boating. Boating damage usually happens when a boat propeller stirs the submerged vegetation or hits the bay bottom. Propeller scars are believed to cause direct loss of seagrass; as well, boat propellers can excavate sediments within channels, which may form berms channels and consequently bury adjacent seagrass, causing mortality and increased susceptibility of seagrass beds to hurricane damage (Hallac, D. E. et al, 2012). Thus, a better understanding about patterns of seagrass scarring as well as its associated physical and human factors of can contribute to management strategies that aim at minimizing resource loss and environment degradation in coastal areas.

Studies on influence of propeller scars on seagrasses have been conducted in many coastal areas including Florida Bay in Everglades National Park, Gulf Coast of Texas, Puerto Rico and Bahama (Hallac, D. E. et al, 2012; Green, K., & Lopez, C., 2007; Uhrin, A. V., & Holmquist, J. G., 2003; Dierssen, H. M. et al., 2003). Mainly using airborne imagery, scarring was found to be most concentrated in shallow beds near navigational channels and in areas frequently used by boats. There was also evidence showing a lower macrofaunal abundance and biodiversity in propeller scars. However, because of restricted availability of

high spatial resolution imagery, very few studies have been done that track changes in seagrasses over shorter time scales, such as at monthly rates

1.2 Application of Remote Sensing Approach on Seagrass Mapping

Remotely sensed imagery has been widely applied for mapping a variety of habitats, including benthic aquatic vegetation. A study by Fyfe (2003) proved that seagrass species have distinct spectrum signatures in spite of spatial and temporal variation in reflectance, which is a sound basis for seagrass mapping using satellite imagery. Due to the particularities of the shallow water environment, the identification of seagrass is different from that of terrestrial vegetation. By examining both multispectral and hyperspectral imagery (including Landsat TM, QuickBird, CBERS, WorldView-2, etc.), the spectral signature of seagrass species showed characteristic features in wavelengths at 530–580 nm, with additional discrimination at 520–530 nm and 580–600 nm; in the red chlorophyll absorption trough at 686 –700 nm; and in the near-infrared (NIR) band at 720 – 900 nm (Fyfe, S. K., 2003 & Manessa, M. D. M. et al., 2014). More specifically, bands at 555, 635, 650 and 675 nm were found to be sensitive to general leaf area index (LAI) (Yang, D. et al. 2009). Dozens of vegetation indices were also tested for better discrimination of presence, percentage of cover, and even species of seagrass (Yang, D. et al., 2009 & Pu, R. et al., 2015), which also provided referential information for methodology exploration for large area seagrass mapping.

The proliferation of drones, also known as unoccupied aircraft systems (UAS), has led to an increasing use in diverse fields of environmental studies in recent decades. Although there have been some ecological applications using ultrahigh-resolution imagery acquired by drones, such as evaluating the vegetation dynamics and forest biodiversity, wildlife conservation, and mapping riparian habitats, a smaller number of applications in monitoring and classification of submerged habitats have been conducted, particularly for submerged vegetation (Ventura, D. et al., 2017). A study conducted in temperate Mediterranean coasts has successfully mapped the extent of a *Posidonia oceanica* meadow

with the purpose of detecting impacted region, and characterizing juvenile fish nursery habitats using drone aerial images integrated with underwater visual census data (Ventura, D. et al., 2017). Applications of drone imagery also show promising prospects in two intertidal sites in Wales, UK. Based on a comparison of classification methods, researchers assessed spatial patterns of intertidal seagrass meadows, as well detection of other biotic features (Duffy, J.P. et al., 2017). However, there has been no published research to date evaluating the temporal change of seagrasses. Thus, the primary dataset used in this study, monthly drone images spanning the growing season, will be analyzed to reveal patterns of disturbance and recovery of seagrass.

1.3 Edge Effect of Habitat Fragmentation

Habitat fragmentation generally refers to a phenomenon in which an intact habitat is segmented into a number of smaller patches separated from each other (Wilcove et al., 1986). Species in these fragmented habitats may be confronted with issues including habitat area decrease, community isolation, and newly induced boundaries (Ewers, R. M., & Didham, R. K., 2006). These modified environments can consequently cause ecological effects on not only species surviving in the habitat remnants, but also the integrity of the habitat itself.

The increase of the amount of habitat edge is one of the most common features of habitat fragmentation. Proliferation of habitat edges can increase the exposure of plant and animal populations to ecological disturbance (Wilcove et al., 1986). Although edge effects in fragments are highly diversified (Laurance, W. F., & Yensen, E., 1991), a number of studies have provided examples of common edge effects: change of microclimate and light regimes influence seedling germination and shade-intolerant plants' survival (Ranney et al., 1981; Lovejoy et al., 1986); more treefalls and higher mortality near edges of forest due to increased wind-shear forces (Levenson, 1981; Lovejoy et al., 1986); birds and mammals are more susceptible at edges by predators, competitors or parasites from outside of habitat (Sievert & Keith, 1985; Andren & Angelstam, 1988). Although the lack of empirical experiments of edge effects on seagrass is an

issue for this study, based on the literature one could hypothesize that seagrass next to propeller scars has been more exposed to water-shear forces and grazed by plankton, than undisturbed beds of seagrass.

1.4 Project Objectives

The goal of this study is to explore methods for seagrass mapping based on a variety of remote sensing products, and evaluate the impact on seagrass from human activities (specifically focused on boat propellers), using ultrahigh-resolution UAS imagery. The main objectives include: a) Classifying seagrasses versus bare benthic beds in UAS images based on automated classification methods. b) Evaluating seagrasses habitat area change over time with/without propeller damage. c) Exploring the factors that influence propeller scar recovery. d) Identifying large-areas of seagrass in high-resolution satellite-based multispectral images.

2. Methods

2.1 Study Site

The study area is part of Core Banks barrier islands (lat/lon 34.67, -76.50) in Beaufort, NC (Figure 1). The satellite imagery covers approximately 26 km² (bottom left), and the UAS imagery covers about 0.7 square kilometers (right). The land cover types within the study area include beach, dunes, maritime forest, salt marsh, mud flats and seagrass beds.

Seagrass beds in Core Banks are primarily composed of three species: widgeon grass (*Ruppia maritima*), shoal grass (*Halodule wrightii*), and eel grass (*Zostera marina*). Widgeon grass predominantly exists in this area most time of year; the main growth season of shoal grass is around March/April-November, and eel grass mainly grows from February – August (Michael A. Mallin et al., 2004).

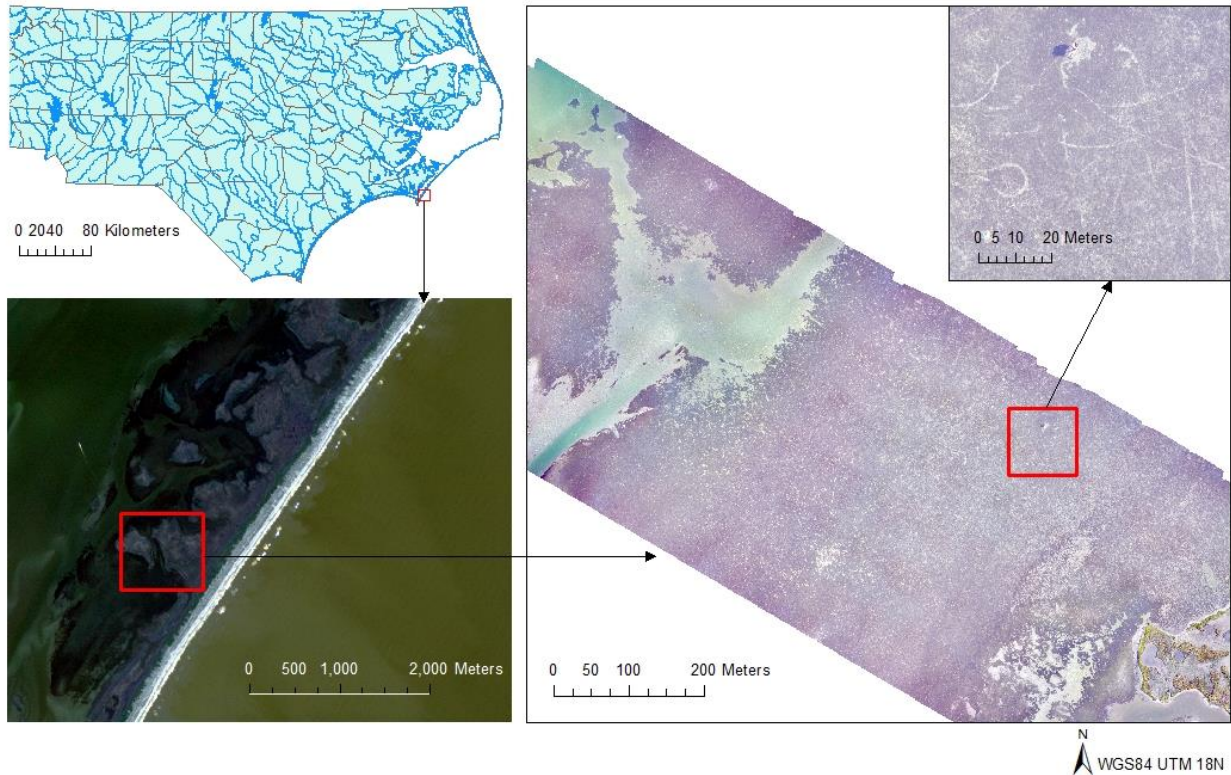


Figure 1. Map of study area. (Top left: boundaries and major rivers in North Carolina; Bottom left: RapidEye image used in this study; Right: an example of UAS images used in this study, with a zoom-in subset showing propeller scars)

2.2 Data Description

2.2.1 Drone-Surveyed RGB Mosaics

The UAS imagery used in this study consists of four RGB mosaics collected in June 14th, July 12th, September 13th and October 19th, 2017. The pixel resolution of the RGB mosaic is typically 0.025 - 0.030 m, with less than 5 cm absolute horizontal and vertical error. The mosaic was georeferenced using survey-grade image geotags and 10 ground control points. Images were collected by eBee plus aircraft and processed by Pix4D Desktop version 3.3 and 3.4. Pix4D performed keypoint matching at "1/2 scale image resolution", and used the "Alternative" camera calibration approach.

2.2.2 High Resolution RapidEye Satellite Imagery

RapidEye Ortho Tile Products are obtained from Planet.com (Planet Team, 2017). The satellite imagery used in this study is a subset of a RapidEye Ortho Tile Product collected September 13th, 2017. These products are radiometrically-, sensor- and geometrically-corrected. The pixel size of imagery is 5 m, after orthorectification using GCPs and fine DEMs (with a post spacing of 30-90 m). Each RapidEye image contains five bands: Blue (0.4750 μm), Green (0.5550 μm), Red (0.6575 μm), Red-edge (0.7100 μm), and Near Infrared (0.8050 μm).

Note that the selection of RapidEye image took into account the influence of tides. As water can partially absorb and scatter electromagnetic radiation, the surface water will affect the identification and classification of below-water objects. Thus, the image values collected during the lowest water level period in the study area will be less influenced by water absorption. According to the nearest NOAA's Center for Operational Oceanographic Products and Services (CO-OPS) Station at Beaufort, NC (Station ID: 8656483; lat/lon: 34.72, -76.67), the water level in the Beaufort coastal area generally reaches its lowest level around 8 am and 9 pm every day. However, all available RapidEye images provided by the Planet Platform are acquired around 12 pm, which is not the worst conditions, yet may introduce errors into the analysis. Since this error is inevitable, the image available on the same date as the UAS image was selected (12:10:51 pm, September 13th). At that moment, the water level of Beaufort station was 1.05 m (Figure 2).

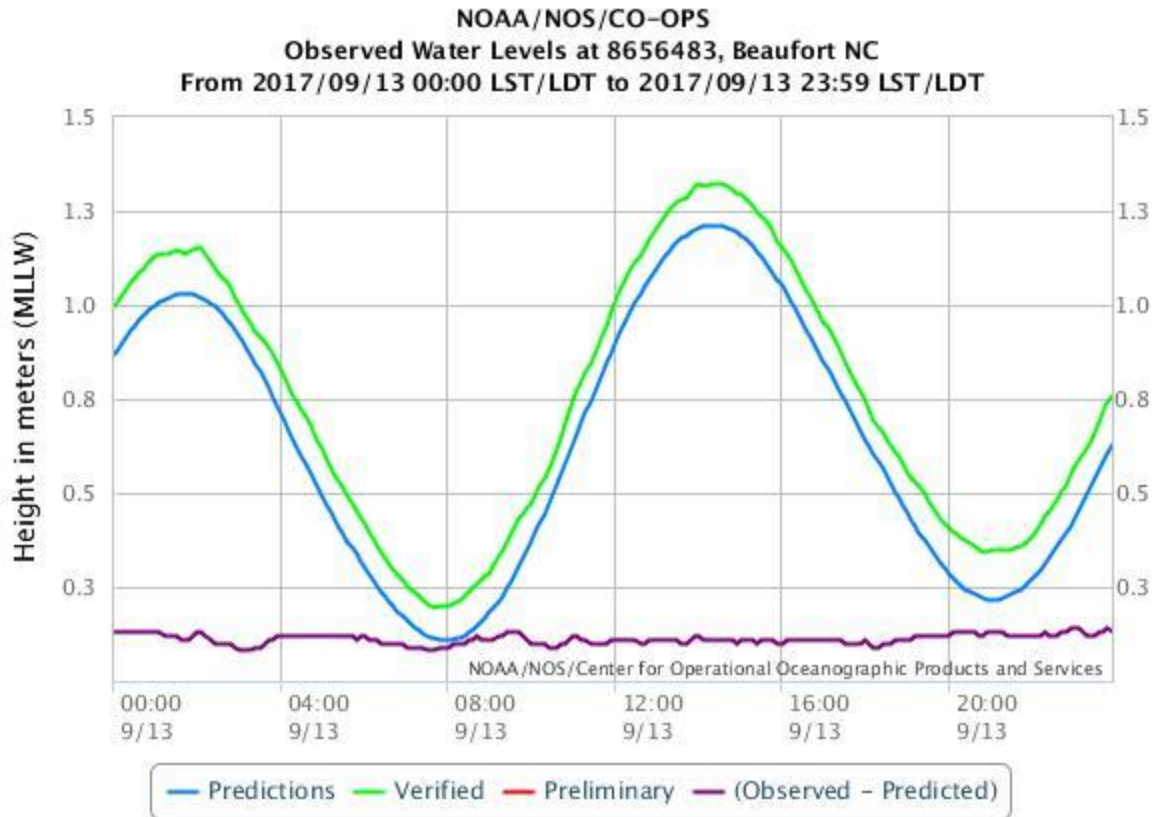


Figure 2. Observed water level at Beaufort station during 2017/09/13.

2.3 Analyses

The primary focus of this project is the classification of seagrass versus non-seagrass. Firstly, four UAS images used in this study were classified individually using object-based classification. After obtaining classified binary images (seagrass/non-seagrass), propeller scars with other bare patches were extracted as a vector file. Based on the result of extracted non-seagrass areas, study area was divided into two classes: area within 3 m – buffer zone of scars were categorized as scar-affected areas, and other areas were treated as non-affected areas; percentage coverage of seagrass in four months were calculated to examine the effect of propeller scars and other bare patches. Although radiometric correction is an available technique for UASs, available images used in the study were not able to perform appropriate correction

upon survey process. So instead of quantitative thresholding, a qualitative exploration on initial conditions of propeller scars recovery was conducted using uncorrected UAS images and relative normalization. The last section of this study is large-area seagrass identification based on high-resolution multispectral satellite imagery. Several new combinations of bands was tested, and one was selected as the proxy to identify only seagrass areas.

Image classification and spectral processing were performed in ENVI 5.4; other spatial analysis was implemented in ArcGIS Desktop 10.5. All images were processed and analyzed in WGS84 datum with UTM projection.

2.3.1 Object-Based Image Classification

Object-oriented image classification can firstly group individual pixels into objects or segments according to their spectral similarity or external rules, which allows for the incorporation of shape and context, as well as user's knowledge into the delineation of habitat boundary. It is a powerful tool for classification of moderate to high resolution data. Utilization of automated segmentation algorithms to create polygons, coupled with CART analysis to develop rules for labeling polygons, brought more details and higher accuracy and consistency to the final product that cannot be obtained using manual interpretation (Green, K., & Lopez, C., 2007). An Object-Based Image Analysis (OBIA) method was applied to classify original images into binary seagrass habitat images; accuracy assessment was then performed to evaluate the classification effectiveness.

2.3.2. Edge-Effect Analysis

In this section, propeller scars and bare patches were processed separately. Since the seagrass coverage in June was considered as initial conditions in this study, both propeller scars and bare patches were extracted using the UAS image collected in June. Bare patches were extracted using the Region Group tool in ArcGIS, which aggregated non-seagrass pixels and removed the aggregations smaller than a certain number of pixels. Propeller scars were identified as polylines manually. Then a 3m-buffer zone

was delineated based on the proximity to extracted scar areas. The results of this step were the masks of two study region types: scar-affected areas or non-affected areas.

The percentage coverage of seagrass in two types of study regions in four months were calculated based on binary seagrass images using Zonal Statistics tool in ArcMap.

2.3.3. Recovery Conditions Exploration

Since available UAS images only have three bands (R, G, B) and were difficult to be radiometric-corrected given known information, the exploration of recovery initial conditions were conducted through relative comparison of RGB-based indices. Visible Atmospheric Resistant Index (VARI) was proposed by Gitelson, A. A. et al at 2002 (Equation 1), aimed to monitor the leaf-area index (LAI) in later stage crops; Triangular Greenness Index (TGI) was created by Hunt, E. R. et al at 2013 (Equation 2), intended to monitor chlorophyll (also nitrogen, indirectly) content of leaves. Both of them only use the visible bands, so they can be created with commonly used cameras and mass-produced consumer drones (McKinnon, T., & Hoff, P., 2017).

$$VARI = \frac{R_{GREEN} - R_{RED}}{R_{GREEN} + R_{RED} - R_{BLUE}} \quad (1)$$

$$TGI = R_{GREEN} - 0.39 * R_{RED} - 0.61 * R_{BLUE} \quad (2)$$

By preliminary examining of VARI and TGI image in a small subset area in all four UAS images, TGI images show relatively more serious distortion than VARI images caused by exposure problems. Hence, VARI was chosen as a proxy for the amount of seagrass.

Within the four-month overlapping area, 28 propeller scars were visually identified and selected according to following criteria: already existing in April, appearing in overlapping area of all four months' images, and not located in areas where suffer from significant exposure problems. By

comparison with the images in June and in October, these 28 propeller scars were categorized into three recovery level: 9 completely recovered (Level 1), 8 partially recovered (Level 2) and 11 non-recovered (Level 3). 2-m buffer zone were built along both sides of each scar, and the VARI values of pixels within each class of buffer zone were calculated using Zonal Statistics tool (Figure 3). To make more sense of these numbers, they are normalized by seagrass areas obtained in 2.3.1, assuming seagrass quantity is linear correlated with seagrass coverage area, and the conditions of this small subset area are identical to anywhere else in this region.

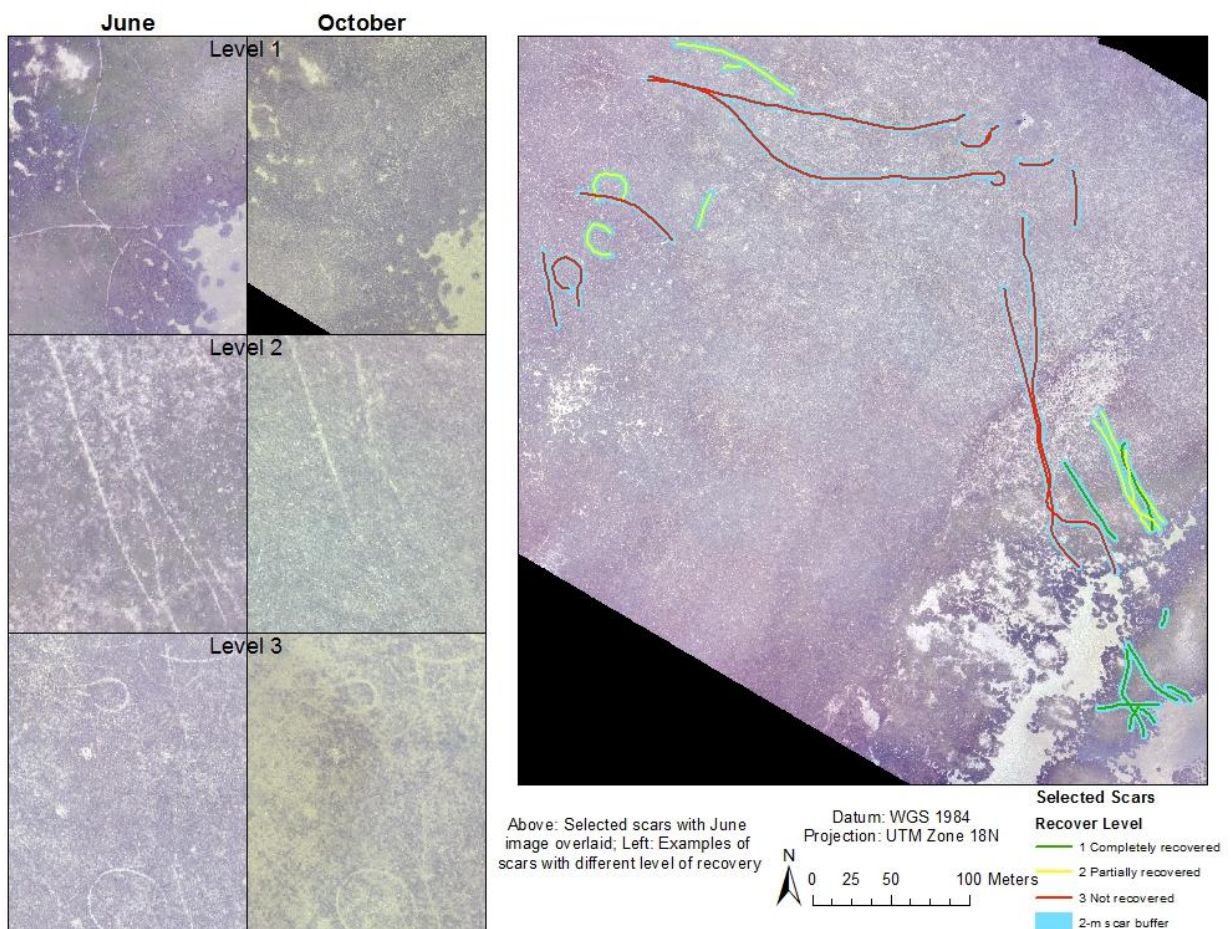


Figure 3. Comparison of categorized propeller scars. Left side shows the examples of scars' comparison between June and October with different level of recovery (1: Completely recovered; 2: Partially recovered; 3: Not recovered). Right side shows the selected scars overlaying on the drone image in June.

2.3.4 Large Area Seagrass Identification

Yang, D. et al (2009) explored viable spectrum and band combinations for seagrass detection in Xincun Bay of Hainan, China, using both multispectral and hyperspectral imagery from a variety of satellites. They found green, red and red-edge spectrum are sensitive to LAI, and Green NDVI (GNDVI) is more sensitive than Red NDVI (RNDVI) and Blue NDVI (BNDVI) in seagrass remote sensing. The equations are:

$$\text{RNDVI} = (\text{NIR}-\text{Red})/(\text{NIR}+\text{Red}) \quad (3)$$

$$\text{GNDVI} = (\text{NIR}-\text{Green})/(\text{NIR}+\text{Green}) \quad (4)$$

$$\text{BNDVI} = (\text{NIR}-\text{Blue})/(\text{NIR}+\text{Blue}) \quad (5)$$

Inspired by these findings, four band combinations were tested in this study: NDVI, Green NDVI (GNDVI), Red-edge NDVI (ReNDVI), and Green+Red-edge NDVI (GReNDVI). The last two indices are computed as follows:

$$\text{ReNDVI} = (\text{Red edge}-\text{Red})/(\text{Red edge}+\text{Red}) \quad (6)$$

$$\text{ReGNDVI} = (\text{Red edge}-\text{Green})/(\text{Red edge}+\text{Green}) \quad (7)$$

By comparing the spectral histogram, the best combination, which is able to optimally separate the seagrass, is used to identify the entire study area. Based on this index image, thresholds are determined visually to delineate the boundary for seagrass.

3. Results

3.1 Ultrahigh-Resolution Seagrass Mapping

OBIA was performed using Rule-based Classification in ENVI (rule parameters are attached in Supplementary Materials). Classified binary images showed increased seagrass coverage from June to July, and then seagrass continuously declined in September and October (Figure 4, 5).

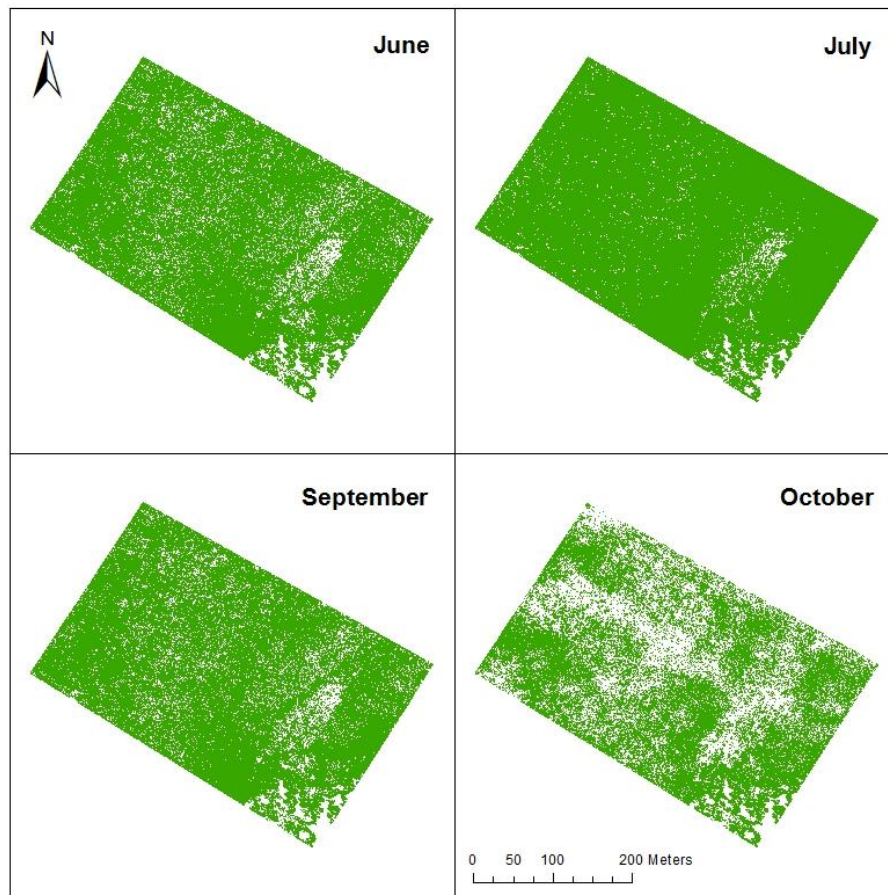


Figure 4. Classified binary seagrass images for four months (pixels in green are seagrass)

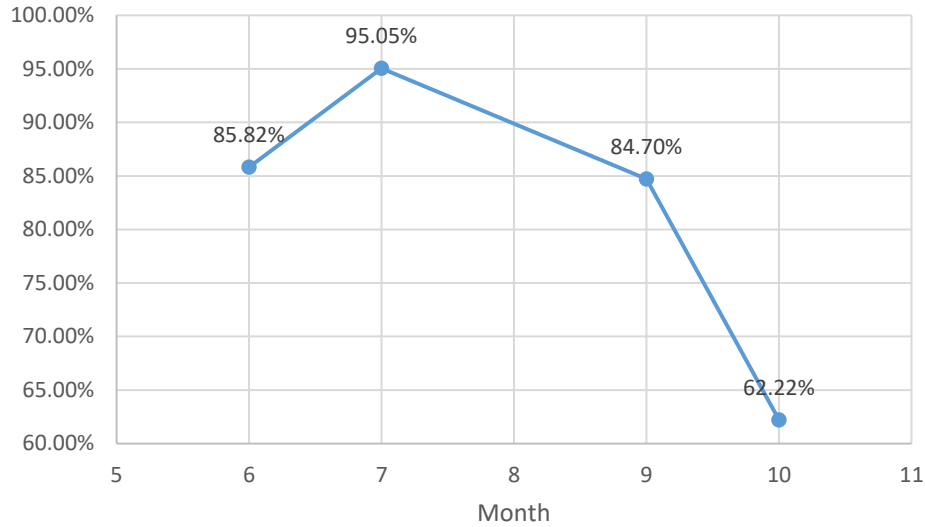


Figure 5. Changes of seagrass coverage within 113620-m² study area over time in 2017

In order to evaluate the accuracy of classification, four binary images are validated by comparing with original images. Each classification image was validated using ~150 random scattered points, and the error matrices indicate this classification method has fairly good results (Table 1).

Table 1. Accuracy assessment matrix of classified images in four months

Month	June	July	September	October
Total Accuracy	91.56%	89.03%	86.45%	79.58%
User's Accuracy	99.20%	89.66%	88.15%	90.00%
Producer's Accuracy	91.18%	98.48%	95.97%	80.20%

3.2 Edge Effect Analysis

Since seagrass in July has maximum coverage and in September has already experienced decline, the binary image in June is used as reference to recognize scar areas. As shown in Figure 6, within 113,620m² study area, scar-affected zone covers about 60% (67,265.9m²) while non-affected zone covers about 40% (46354.3m²).

By calculating the percent coverage of seagrass in scar-affected/non-affected regions in four months, the results showed that compared with non-affected regions, seagrass in scar-affected regions has greater rate

of both growth and decline. The results also indicated a fact that propeller scars have more serious impact on seagrass when total amount of seagrass is at lower level. The percentage of impact was lowest in July (7%), but caused the most significant impact in October, explaining up to 20% decline of seagrass (Figure 7).

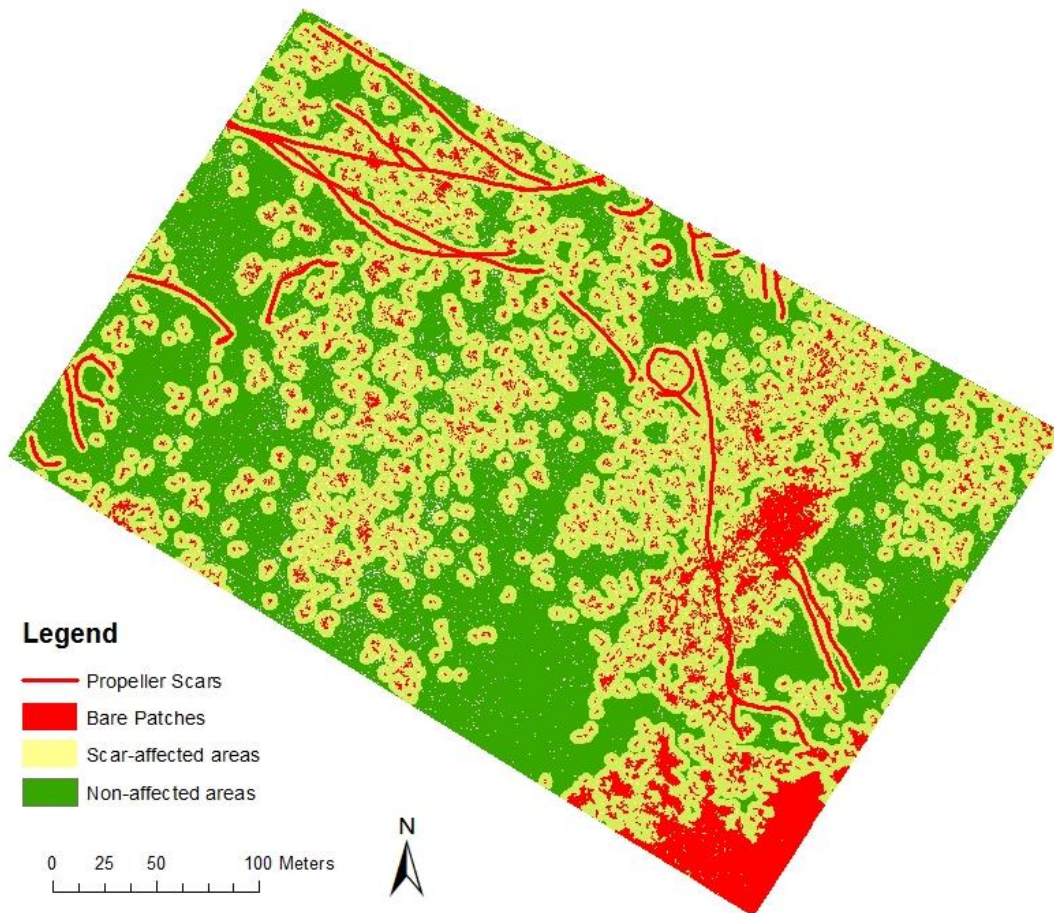


Figure 6. Scar-affected areas versus non-affected areas

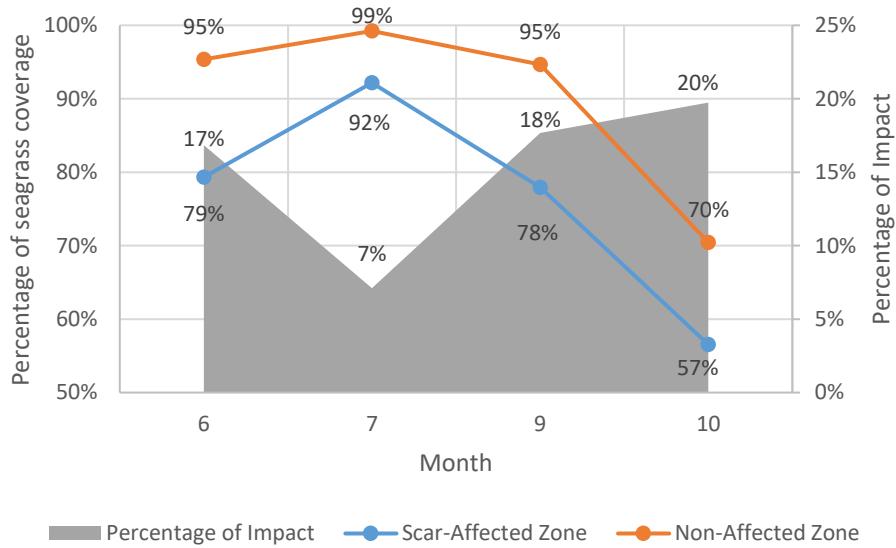


Figure 7. Changes of seagrass coverage in scar-affected/non-affected areas over time

3.3 Recovery Conditions

Area-normalized VARI for different recovery levels show some interesting results (Figure 8). From June to October, VARI of areas in Level 1, completely recovered, is approximately 19% higher than in Level 2 and 3, partially or not recovered, while the Level 2 and 3 areas didn't show significant difference in terms of their recovery speed and timing.

Level 1 areas also have a different peak in the growing season from Level 2 and 3. These areas reach a maximum amount of seagrass in July, but decline dramatically in September until October. Partially or not recovered areas showed increase in seagrass amount slowly until September, then decline in October.

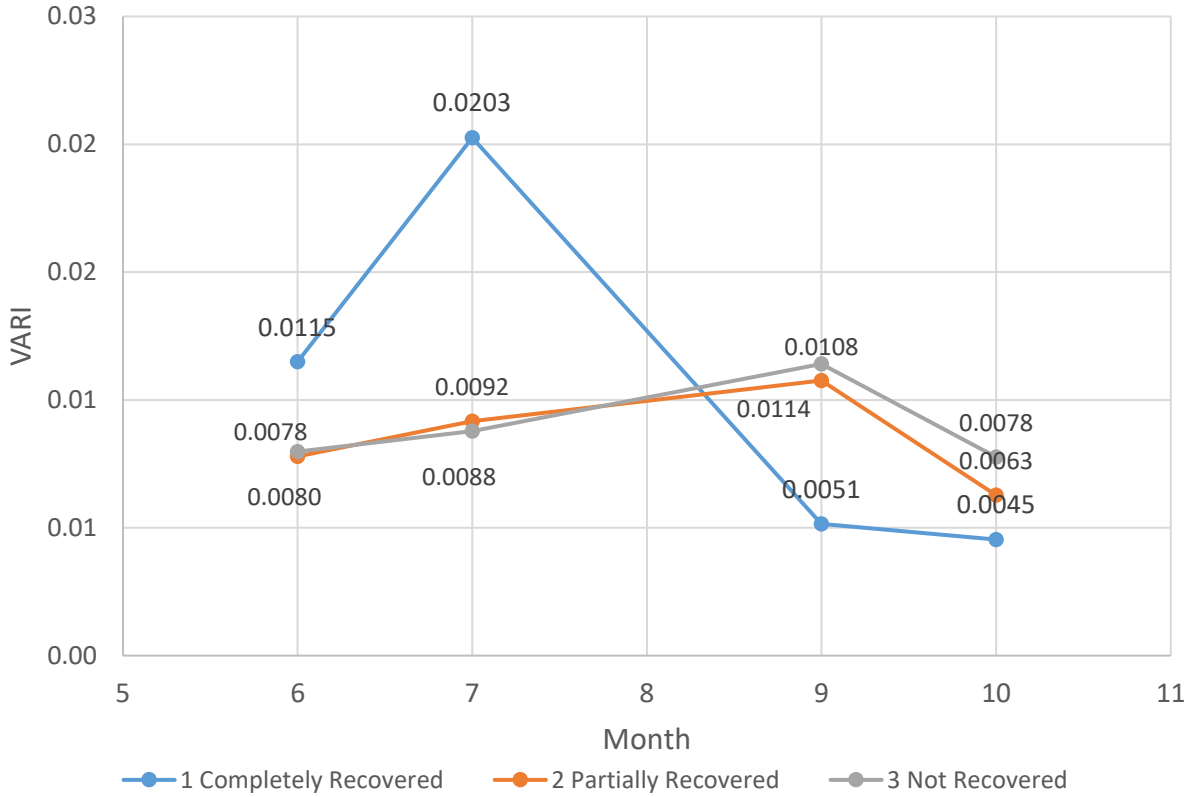


Figure 8. Visible Atmospheric Resistant Index (VARI) of three recovery-level areas in four months

3.4 Seagrass Mapping based on New Index

Using the Maximum Likelihood classification and the UAS image as “ground truth”, a RapidEye image was classified into four classes: sand above water, vegetation (terrestrial), sand below water, and seagrass (Fig. 9 A & B). By similar accuracy assessment methods described in 3.1, this classification was found to have a total accuracy of 83%.

From a spectral histogram (Fig. 10), ReGNDVI appears the most distinctive spectral signature for seagrass. Thus, ReGNDVI was used to compute the image for classification. Pixels having values between -0.533 and -0.323 were visually identified as seagrass area (Fig. 9 C). Using the same validation method and the supervised classification (Fig. 9 B) as pseudo-groundtruth, the thresholding classification

resulted in a total accuracy of 86%. If we apply the ReGNDVI transform twice to the original image, and select pixels between 0.170 - 0.278 as seagrass area (Fig. 9 D), this accuracy can be raised up to 89%.

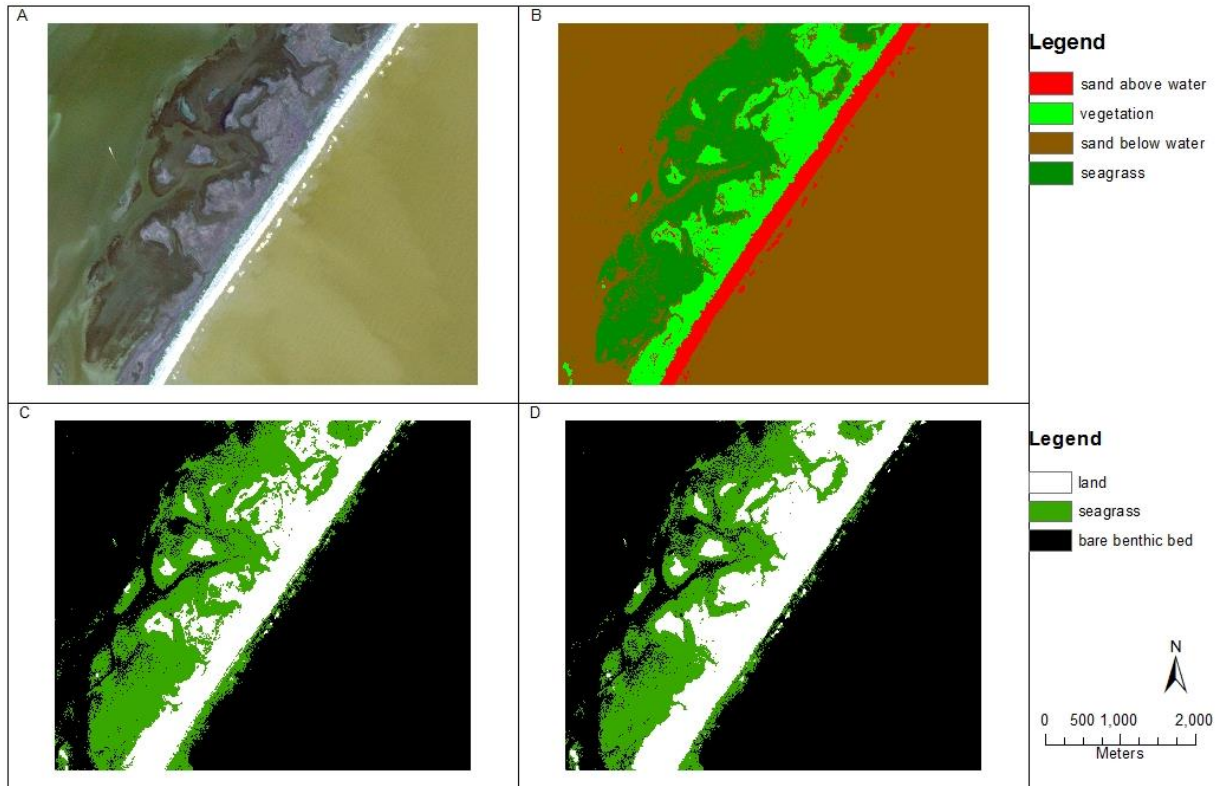


Figure 9. Seagrass mapping using RapidEye imagery A. Original image. B. Supervised-classification result. C. ReGNDVI thresholding result. D. Double ReGNDVI thresholding result.

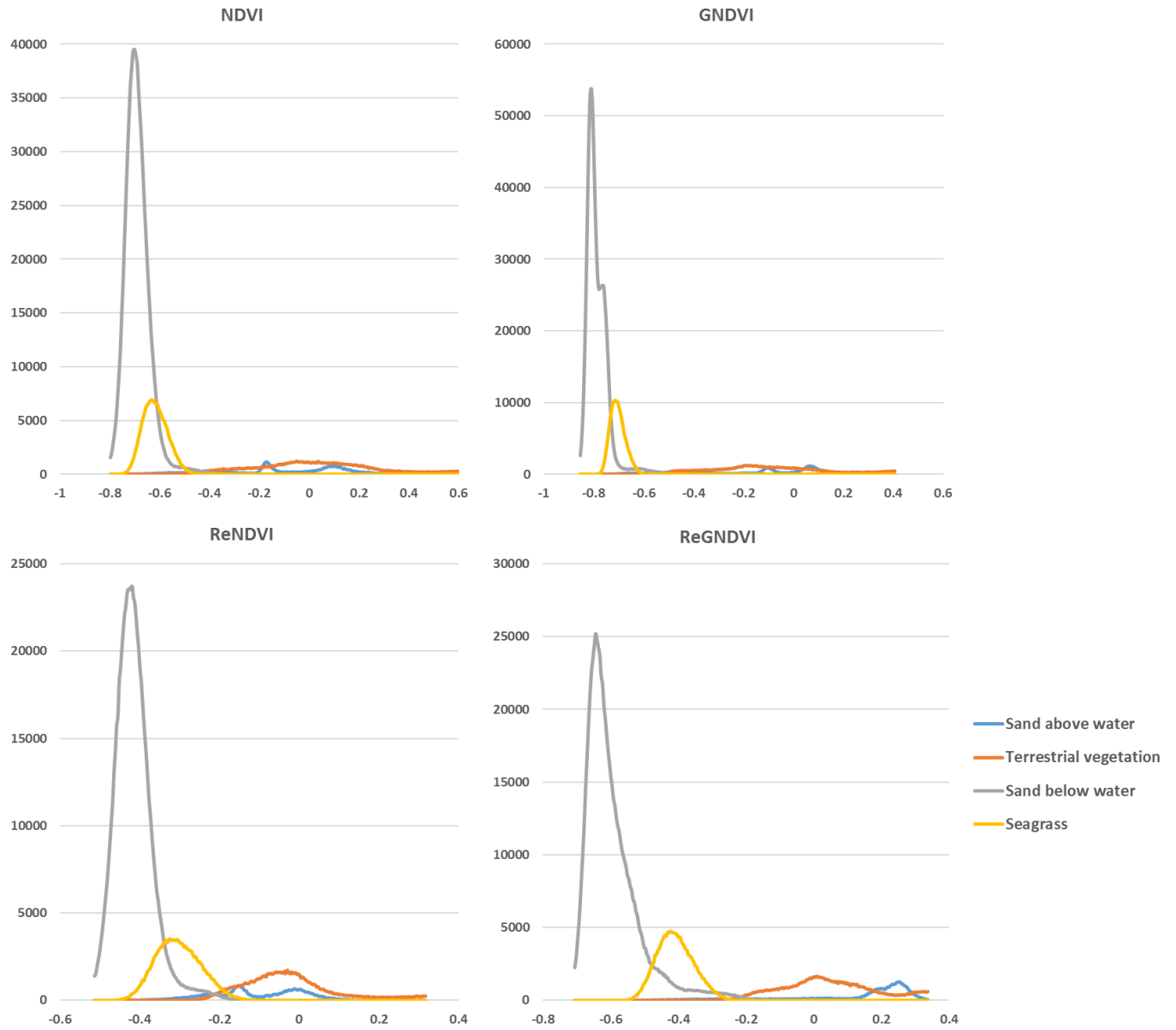


Figure 10. Spectral signature of four classes through NDVI, GNDVI, ReNDVI and ReGNDVI transforms

4. Discussion

4.1 Issues on Analysis Techniques

This project provides a successful application of Object-Based Classification in classifying drone images in coastal submerged areas. The total accuracy of all four classifications were between 80%-90%, which indicates a promising application of OBIA in studies using UAS images. However, lack of appropriate radiometric correction of the imagery introduced various problems in this study. Firstly, the classification parameters for one image cannot be applied to other images without radiometric correction (see Supplementary Materials). It significantly increased cost of time and labor, and would be more serious when processing a number of UAS images. Secondly, the lack of radiometric correction also constrained the information that could have been utilized. The indicators of plant growth usually need various combinations of bands, however, those indices are not comparable among images if they are not corrected to a similar baseline.. In this study, a relative radiometric normalization was used as an alternative, but this approach was based on two bold assumptions and consequently has deficiencies. As mentioned in previous sections, radiometric correction is already an available technique for UASs, so the intention here is to emphasize the importance of conducting radiometric correction during UAS surveys.

Another issue reducing the imagery quality is exposure problems. Some images suffering from bright and dark exposure strips in a certain (or several) single band images running through the study area. It does not impede the visual identification of seagrass versus bare beds, but leads to a lower accuracy of classification as well as growth index comparison. For instance, the classification of the October image has the lowest accuracy, which is mostly because of significant exposure problem. With closer examination of the random points for accuracy assessment, most of the false negative points are located in areas with radiometric distortion, while most of false positive points are scattered in areas of geometric distortion. Exposure problems are difficult to fix during post processing, so it requires more caution and planning during drone's deployment.

Feature extraction in this project was a combination of an automated approach for bare patches extraction, and manual approach for scar line extraction. Manual extraction is not a big problem when the study area is a small region, but would be troublesome for larger study area. Thus, an automated approach to scar line extraction is still an interesting topic to explore, which indicates a potential of interdisciplinary study between remote sensing and image recognition.

Available bands of imagery is also a bit concern for these types of studies. Since UAS images used in this project only have three bands (R, G, B), many widely applied vegetation indices that rely on near infrared information, cannot be used (such as NDVI, EVI, etc.). Alternatively, Visible Atmospheric Resistant Index (VARI) was chosen as the proxy of leaf area index, although the performance of VARI has far less verification in ecological studies. On the contrary, seagrass mapping using high-resolution multispectral satellite imagery (e.g. RapidEye collections) showed a promising result in terms of large area seagrass identification, taking advantage of its unique red-[near-infrared] edge band. The classification accuracy could be improved by adapting other data sources with higher spectral resolution (such as WorldView collections) or more band combinations. This indicates the potential of large area seagrass mapping using high-resolution multispectral satellite imagery, and also provides a new approach in coastal habitat conservation.

4.2 Discussion on Seagrass Recovery

It is not surprising that seagrass decline appears to be faster in scar-affected areas compared to non-affected areas. Many previous studies have indicated that decline of habitat is more likely to appear at the edges, and therefore fragmentation may accelerate habitat loss. Meanwhile, I also found that it appears seagrass in scar-affected areas recovers faster than non-affected areas during the growing season. Possible reasons for this finding can be that seagrass is easier to be found in areas where it is sparse, and seagrass tends to spread to its surrounding areas. Nonetheless, more convincing conclusion needs field experiments or empirical data.

The factors influencing seagrass recovery still need discussion. The VARI of Level 1 is approximately 19% higher than Level 2 and 3, while the Level 2 and 3 areas didn't show significant difference in terms of their recovery speed and timing. Level 1 areas also have different peak growth season from Level 2 and 3. These areas reach maximum amount of seagrass in July, but decline dramatically in September until October. Partially or not recovered areas increase seagrass amount slowly until September, then decline in October.

Based on given knowledge about this area, two possible reasons might explain this finding. The first is initial condition matters - the scars that appear in areas with higher density of seagrass (Level 1 is about 43% higher than Level 2 and 3 in June) are more likely to recover. Higher density of seagrass has the ability to form more stable habitats, and consequently may have stronger resilience. The second explanation is the role of different species. VARI of the level 1 affected area drops dramatically from July to September, which indicates a possibility that these areas have relatively higher percentage of eel grass; the major growth season of eel grass is from Feb to Aug. However, this hypothesis needs further confirmation with on-the-ground sampling, as previous studies have shown that this area is dominant by widgeon grass which usually grows most of year.

5. Conclusions

This study provides a successful application of Object-Based Classification in classifying coastal submerged areas in UAS images, showing that UAS techniques have potential in monitoring submerged areas as well as conservation of coastal habitats. However, the performance of UASs depends on a series of related techniques, especially radiometric correction and spectral resolution. These issues should be addressed in planning stage of similar research or conservation work.

Through the analysis on propeller scars' impact on seagrass, human activities have been proven to have lasting effects on seagrass habitat, since seagrass in scar-affected regions has greater rate of both growth

and decline. The scars appearing in areas with higher density of seagrass are more likely to recover, although this conclusion needs further confirmation with on-the-ground species composition data. This finding can be a suggestion for coastal management that human activities should be restricted in vulnerable seagrass habitats, and necessary boating or fishing pass way should only be allowed in areas with high-density of seagrass, since these areas are less susceptible to propeller scars.

In addition, this study also shows that automated seagrass mapping is feasible using high-resolution satellite imagery (e.g. RapidEye) and a newly developed index, ReGNDVI (Red Edge-Green NDVI). It has potential for large-area seagrass mapping, and might be useful for conservation of coastal areas.

Acknowledgement

First of all, I would like to thank my advisor, Dr. Jennifer Swenson, for her suggestions on finding technical solutions and continuous support; without her help I would not see the progress from zero to a complete project. I also want to thank Dr. Ram Oren, for his comments on making analysis more robust and more ecologically meaningful.

The UAS images were provided by Marine Robotics and Remote Sensing Group in Duke University Marine Lab. I would like to express my great appreciation to Alexander Seymour, who introduced UAS technique to me and gave me many useful suggestions on image processing. Thanks to Dr. Dave Johnston and people who helped with drone survey and made data available to me; without these images I could not made this project happen.

Finally, thanks to my parents, for their unconditional love and support throughout my study at the Nicholas School.

References

- Andren, H., & Anglestam, P. (1988). Elevated predation rates as an edge effect in habitat islands: experimental evidence. *Ecology*, *69*(2), 544-547.
- Dierssen, H. M., Zimmerman, R. C., Leathers, R. A., Downes, T. V., & Davis, C. O. (2003). Ocean color remote sensing of seagrass and bathymetry in the Bahamas Banks by high-resolution airborne imagery. *Limnology and oceanography*, *48*(1part2), 444-455.
- Duarte, C. M., Marbà, N., & Santos, R. (2004). What may cause loss of seagrasses. *European seagrasses: an introduction to monitoring and management*, 24.
- Duffy, J. P., Pratt, L., Anderson, K., Land, P. E., & Shutler, J. D. (2017). Spatial assessment of intertidal seagrass meadows using optical imaging systems and a lightweight drone. *Estuarine, Coastal and Shelf Science*.
- Ewers, R. M., & Didham, R. K. (2006). Confounding factors in the detection of species responses to habitat fragmentation. *Biological reviews*, *81*(1), 117-142.
- Fyfe, S. K. (2003). Spatial and temporal variation in spectral reflectance: Are seagrass species spectrally distinct? *Limnology and Oceanography*, *48*(1part2), 464-479.
- Gitelson, A. A., Kaufman, Y. J., Stark, R., & Rundquist, D. (2002). Novel algorithms for remote estimation of vegetation fraction. *Remote sensing of Environment*, *80*(1), 76-87.
- Green, K., & Lopez, C. (2007). Using object-oriented classification of ADS40 data to map the benthic habitats of the state of Texas. *Photogrammetric Engineering and Remote Sensing*, *73*(8), 861.
- Hallac, D. E., Sadle, J., Pearlstine, L., Herling, F., & Shinde, D. (2012). Boating impacts to seagrass in Florida Bay, Everglades National Park, Florida, USA: links with physical and visitor-use factors and implications for management. *Marine and Freshwater Research*, *63*(11), 1117-1128.
- Hunt, E. R., Doraiswamy, P. C., McMurtrey, J. E., Daughtry, C. S., Perry, E. M., & Akhmedov, B. (2013). A visible band index for remote sensing leaf chlorophyll content at the canopy scale. *International Journal of Applied Earth Observation and Geoinformation*, *21*, 103-112.
- Laurance, W. F., & Yensen, E. (1991). Predicting the impacts of edge effects in fragmented habitats. *Biological conservation*, *55*(1), 77-92.
- Levenson, J. B. (1981). Woodlots as biogeographic islands in southeastern Wisconsin. *Forest island dynamics in man-dominated landscapes*, 13-39.
- Lovejoy, T.E., Bierregaard, R.O., Rylands, A. B., Malcolm, J. R., Brown, K.S., Quintela, C.E., Harper, L.H., Powell, A.H., Powell, G.V.N., Schubart, H. O. R. & Hays, M. B. (1986). Edge and other effects of isolation on Amazon forest fragments. In *Conservation Biology: The Science of Scarcity and Diversity*, ed. M.E. Soulé. Sinauer Associates, Sunderland, Massachusetts, pp. 257-85.
- Manessa, M. D. M., Kanno, A., Sekine, M., Ampou, E. E., Widagti, N., & As-syakur, A. R. (2014). Shallow-water benthic identification using multispectral satellite imagery: investigation on the effects of improving noise correction method and spectral cover. *Remote Sensing*, *6*(5), 4454-4472.
- McKinnon, T., & Hoff, P. (2017) Comparing RGB-Based Vegetation Indices with NDVI For Drone Based Agricultural Sensing. Agribotix, LLC 2017 (Agribotix.com)

Michael A. Mallin, Virginia L. Johnson, Matthew R. McIver. (2004). Assessment of Coastal Water Resources and Watershed Conditions in Cape Lookout National Seashore North Carolina. Technical Report NPS/NRWRD/NRTR-2004/322. <http://www.uncw.edu/cmsr/aquaticceology/laboratory>

Orth, R. J., Carruthers, T. J., Dennison, W. C., Duarte, C. M., Fourqurean, J. W., Heck, K. L., ... & Short, F. T. (2006). A global crisis for seagrass ecosystems. *AIBS Bulletin*, 56(12), 987-996.

Planet Team (2017). Planet Application Program Interface: In Space for Life on Earth. San Francisco, CA. <https://api.planet.com>

Pu, R., Bell, S., & English, D. (2015). Developing hyperspectral vegetation indices for identifying seagrass species and cover classes. *Journal of Coastal Research*, 31(3), 595-615.

Ranney, J. W., Bruner, M. C., & Levenson, J. B. (1981). Importance of edge in the structure and dynamics of forest islands. *Ecological studies; analysis and synthesis*.

Sievert, P. R., & Keith, L. B. (1985). Survival of snowshoe hares at a geographic range boundary. *The Journal of wildlife management*, 854-866.

Uhrin, A. V., & Holmquist, J. G. (2003). Effects of propeller scarring on macrofaunal use of the seagrass *Thalassia testudinum*. *Marine Ecology Progress Series*, 250, 61-70.

Ventura, D., Bonifazi, A., Gravina, M. F., & Ardizzone, G. D. (2017). Unmanned Aerial Systems (UASs) for Environmental Monitoring: A Review with Applications in Coastal Habitats. In *Aerial Robots- Aerodynamics, Control and Applications*. InTech.

Wilcove, D. S., McLellan, C. H., & Dobson, A. P. (1986). Habitat fragmentation in the temperate zone. *Conservation biology*, 6, 237-256.

Yang, D., & Yang, C. (2009). Detection of seagrass distribution changes from 1991 to 2006 in Xincun Bay, Hainan, with satellite remote sensing. *Sensors*, 9(2), 830-844.

Supplementary Materials

Parameters used in Rule-Based Classification

Month	June	July	September	October
Segmentation Algorithm	Intensity	Intensity	Intensity	Intensity
Segment Value	0.00	0.00	0.00	0.00
Segment Bands	1,2,3,4	1,2,3,4	1,2,3,4	1,2,3,4
Merge Algorithm	Full Lambda Schedule	Full Lambda Schedule	Full Lambda Schedule	Full Lambda Schedule
Merge Value	90.00	90.00	90.00	90.00
Merge Bands	1,2,3,4	1,2,3,4	1,2,3,4	1,2,3,4
Kernel Size	3	3	3	3
Classification Type	Rule-Based	Rule-Based	Rule-Based	Rule-Based
Class Threshold	0.8	0.8	0.8	0.5
Base Name	Spectral Mean	Spectral Mean	Spectral Mean	Spectral Mean
Attribute Value	153.45672	165.52536	152.50421	150.80645